International Conference on Space Optics—ICSO 2008

Toulouse, France

14–17 October 2008

Radiometric packaging of uncooled bolometric infrared focal plane arrays

Sonia García-Blanco

Timothy Pope

Patrice Côté

Mélanie Leclerc

et al.

RADIOMETRIC PACKAGING OF UNCOOLED BOLOMETRIC INFRARED FOCAL PLANE ARRAYS

Sonia Garcia Blanco[1], Timothy Pope[1], Patrice Coté[1], Mélanie Leclerc[1], Linh Ngo Phong[2], and François Châteauneuf[1]

[1]INO, 2740 Einstein St., Quebec, QC G1P 4S4, Canada. francois.chateauneuf@ino.ca
[2]Canadian Space Agency, 6767 route de l'Aéroport, Saint-Hubert, QC J3Y 8Y9, Canada. linh.ngo-phong@space.gc.ca

ABSTRACT

INO has a wide experience in the design and fabrication of different kinds of microbolometer focal plane arrays (FPAs). In particular, a 512x3 pixel microbolometer FPA has been selected as the sensor for the New Infrared Sensor Technology (NIRST) instrument, one of the payloads of the SAC-D/Aquarius mission. In order to make the absolute temperature measurements necessary for many infrared Earth observation applications, the microbolometer FPA must be integrated into a package offering a very stable thermal environment. The radiometric packaging technology developed at INO presents an innovative approach since it was conceived to be modular and adaptable for the packaging of different microbolometer FPAs and for different sets of assembly requirements without need for re-qualification of the assembly process. The development of the radiometric packaging technology has broadened the position of INO as a supplier of radiometric detector modules integrating FPAs of microbolometers inside a radiometric package capable of achieving the requirements of different space missions. This paper gives an overview of the design of INO's radiometric package. Key performance parameters are also discussed and the test campaign conducted with the radiometric package is presented.

1. INTRODUCTION

INO has a wide experience in the design and fabrication of different kinds of uncooled microbolometer focal plane arrays (FPAs). In the context of a development initiated by ESA and completed in collaboration with the Canadian Space Agency (CSA), a 512x3 pixel microbolometer focal plane array for multi-band pushbroom imaging has been developed. This FPA has been selected as the sensor for the New Infrared Sensor Technology (NIRST) instrument [1,2], one of the payloads of the SAC-D/Aquarius mission [3].

In order to make absolute temperature measurements necessary for many infrared Earth observation applications, the microbolometer FPA must be integrated into a package offering a very stable thermal environment. In some missions, frequent offset calibrations of the instrument are not possible and tight control of the detector thermal environment is not always easy. The use of a radiometric package in those applications allows reduced frequency of offset calibration while relaxing the need for temperature control of the system, thanks to the stabilization of the detector environment provided by the radiometric package.

Under the Space Technology Development Program (STDP) of the CSA, INO has designed, assembled and radiometrically characterized a radiometric package. The design of the radiometric package was based on a 512x3 pixel uncooled microbolometer FPA providing for the development of a low weight, low size and low power consumption, sensitive detector package, ideally suited for infrared pushbroom imaging applications.

The radiometric packaging technology developed at INO was conceived to be modular and adaptable for the packaging of different microbolometer FPAs and to address different sets of performance requirements without the need for re-qualification of the assembly process. To that aim, most of the components used in the package are either commercial-off-the-shelf or manufactured at INO and can be easily adapted to enable the packaging of different FPA arrays meeting different optical and performance related requirements (such as numerical aperture, temperature stability, stray light rejection or operating spectral band) without altering the packaging procedure. This approach enables INO to offer its pre-space qualified radiometric packaging technology for different space instrumentation developments.

The design of INO's radiometric package reduces the influence of temperature variations of the environment on the response of the detector. A variation of the ambient temperature of the package of 1 C induces a 0.1 C variation on the apparent scene temperature detected by the sensor. The package also shows a very low sensitivity to stray radiation due to the special design of a very efficient radiation shield. Using the INO/CSA 512x3 pixel microbolometer FPA, an NETD as low as 23 mK (8-12 μm spectral band, 140 ms integration time, f/1 optics, characterization in flood exposure) has been measured. In order to perform the

radiometric tests on Earth, the package is dynamically pumped.

The device has passed successfully critical environmental tests without degradation of its performance, demonstrating its compatibility with the space environment. It has been thermally cycled from -55 to +85 C according to MIL-STD-810, randomly accelerated up to 14 G RMS from 20-2000 Hz and shock tested up to 75 G.

INO's efforts are increasingly focused on space applications using micro-electro-mechanical systems, including uncooled microbolometer FPAs, thin films [4], packaging, and optical design technologies [5]. There is an increasing number of planned Earth and planetary observation missions involving thermal imagers. The development of the radiometric packaging technology has broadened the position of INO as a supplier of radiometric detector modules integrating FPAs of microbolometers inside radiometric packages capable of addressing the requirements of different space missions.

Section 2 gives an overview of the design of INO's radiometric package while the results of the characterization of key performance parameters are described in Section 3.

2. DESIGN OVERVIEW

Figure 1 shows the geometry of the designed radiometric package. The different components of the radiometric assembly are mounted into a custom designed Kovar header the features of which have been designed to ensure mechanical stability of the assembly together with good heat dissipation of the package. Inside the header, a thermo-electric cooler has been incorporated to accurately control the temperature of the bolometric detector, the filter and the radiation shield within 10 mK. Temperature control of the different parts is very important to prevent changes on the background radiation reaching the detector not accounted for by the calibration.

A temperature stabilized radiation shield ensures a stable environment outside the field of view of the microbolometer detector. A shield is especially important for radiometric infrared detection, to minimize the effect of variations of the temperature of the detector environment. In a radiometric measurement, the shield temperature should be either cold (to minimize its emission) or controlled. For an uncooled detector, the shield is usually controlled in temperature.
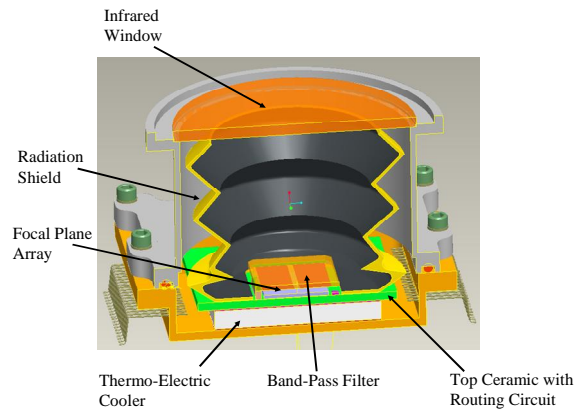
(a)
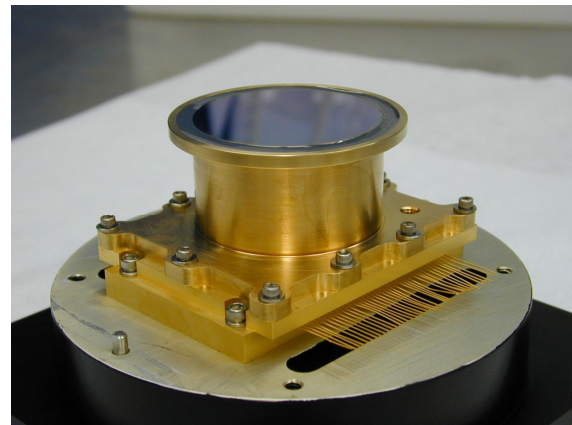
(b)

Figure 1: (a) 3-D view of the radiometric package showing the different components; (b) Picture of the assembled package.

Rays coming at angles outside the numerical aperture of the instrument should not reach the detector. If a radiation shield is not used, most of these rays will fall outside the detector. When a radiation shield is necessary, these rays will hit the radiation shield and can potentially reach the detector by reflection. The design of the radiation shield should be such that the stray rays are absorbed by the shield and do not reach the detector. This is achieved by coating the interior of the shield with an absorbing coating and by designing the shield shape to force parasitic rays to hit as many times as possible the shield internal surfaces before reaching the detector. The outside shield coating should be as reflective as possible to prevent temperature transfer from the exterior of the package to the shield that will induce a variation of the amount of background radiation arriving at the detector not accounted for by the calibration.

Finally, a filter that permits to select the operating spectral bands for the device can also be included in the package.

3. CHARACTERIZATION OF KEY PACKAGE PERFORMANCES

In this section the methodology for the characterization of the different performance parameters (SITF, NETD, robustness to variation of the ambient temperature and to stray radiation) is described. The results obtained using the test campaign are also discussed.

3.1 Signal Transfer Function (SITF) and Noise-Equivalent Temperature Difference (NETD)

The Signal Transfer Function (SITF) is the variation of the response of the detector to a variation of the temperature of the scene. In the measurement of the SITF, the response of the system to two different scene temperatures is measured. The two temperatures should be close to the temperature at which the NETD is required due to the non-linearity of the SITF with the temperature.

In the case of this work, the SITF has been characterized between scene temperatures of 25 C and 35 C for NETD measurements at 30 C. A typical graph of the response of a microbolometer detector line (mean response of the 512 pixels) to a step in the temperature of the scene blackbody between 25 C and 35 C is presented in Figure 2. The response of the detector is measured after the analog to digital converter (ADC) of the Readout Integrated Circuit (ROIC), being therefore given in counts. Its value depends not only on the response of the pixels but also on the different ROIC parameters along the signal transfer chain (such as gain, comparator voltage thresholds, integration time and clock frequency). The SITF is then calculated as

$$SITF = \frac{M_2 - M_1}{T_2 - T_1} \quad [\frac{counts}{C}]$$

for each pixel in the array, where M_2 and M_1 are the mean of the response of each pixel over several acquisitions for temperatures of scene T_2 and T_1.

The Noise Equivalent Temperature Difference (NETD) measures the increment of temperature of the scene that produces a peak signal-to-noise ratio of 1 under flood illumination [6, 7]. For the NETD characterization using the radiometric package, a set of more than 1000 acquisitions were taken at the scene temperature of the measurement. The low frequency component was then eliminated by applying a high-pass filter to the collected data. The RMS of the filtered

data represents the high frequency noise used for the NETD calculation. Another method used for the calculation of the high frequency noise is based on the computation of the Power Spectral Density (PSD) of the temporal data (the noise power spectrum) [8]. The PSD is given in counts^2/Hz and the usual shape shows a 1/f feature followed by a plateau at higher frequencies (Figure 3 (b)). The level of this plateau is used to estimate the instantaneous RMS noise by assuming that it represents the white noise level across the full bandwidth.
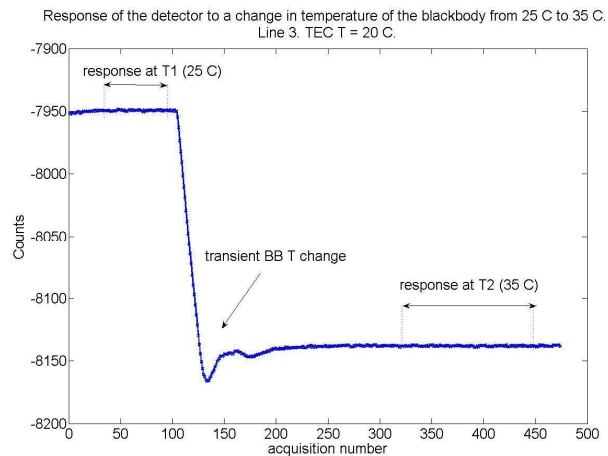

Figure 2: Example of measurement of the mean detector response (over the 512 pixels) to a change of the temperature of the blackbody as a function of acquisition number. The temperature of the blackbody is varied after 100-150 acquisitions. Measurement parameters: Temperature of TEC 20 C, integration time 140 ms, clock frequency 2 MHz.

In the current measurements, the time to collect 1000 acquisitions is 9 min. Therefore, the sampling period is 0.54 sec and the sampling frequency Fs is 1.85 Hz. A "one-sided" "pwelch" function has been utilized. Therefore, all the spectral power is contained in the range of frequencies from 0 Hz to Fs/2 (i.e. 0.93 Hz, the Nyquist frequency). By integrating the noise floor (indicated by a red line in Figure 3 (b)) over the frequency range from 0 Hz to 0.93 Hz, the instantaneous RMS noise can be obtained. Figure 3 (b) shows the PSD of the measured signal shown in Figure 3 (a). The high frequency noise filtered using a high-pass filter is shown in Figure 3 (c).
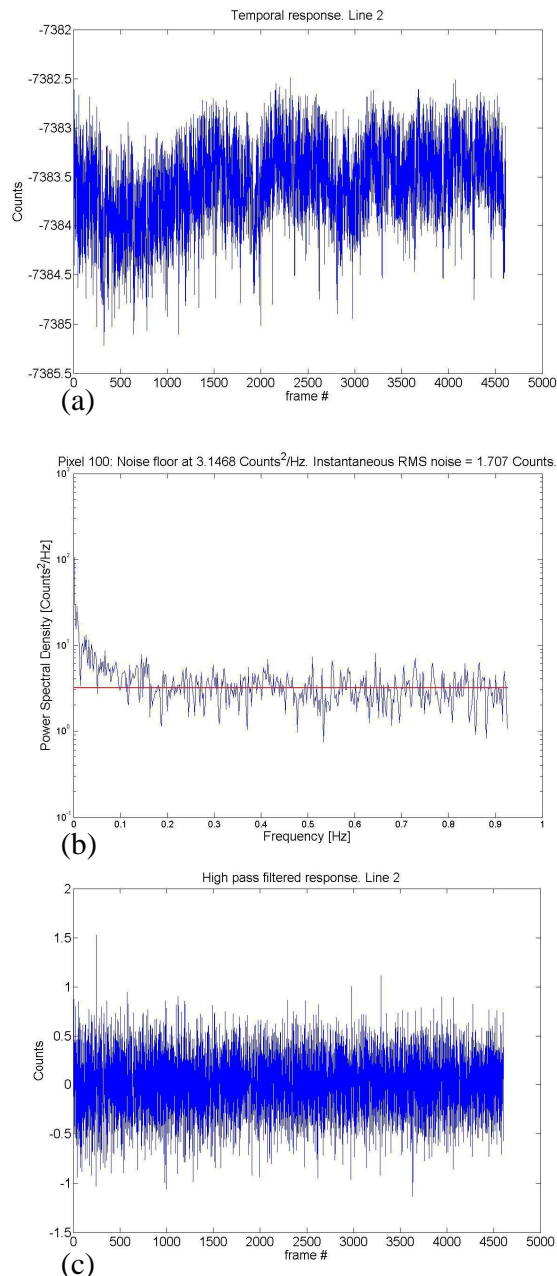
(a)

(b)

(c)

Figure 3: (a) Mean response of the 512 pixels of the line 2 of a microbolometer pixel array to a scene at a constant temperature of 25 C. Collection time for 1000 acquisitions is around 9 min; (b) Power density spectrum of the signal from (a) after removal of the DC component. The white noise level is indicated by the red line; (c) High frequency noise extracted from temporal response raw data from (a). Measurement conditions: Type IIB ROIC 140 ms integration time, 2 MHz clock frequency, TEC T 20 C, BB T 25 C.

The NETD is then calculated as the high frequency temporal noise per pixel divided by the SITF

$$ins\tan\tan eous\ NETD\ = \frac{high\ frequency\ temporal\ noise}{SITF}\ [K]$$

The value of NETD highly depends on the optical components integrated in the package derived from specific mission requirements. Filter spectral band and bandwidth, window transmission, temperature of operation and integration time have an influence on the value of measured NETD. Furthermore, the NETD is also dependent on the temperature of the scene at which it is measured. Therefore, the scene temperature should be specified when reporting a value of NETD.

INO has developed different types of microbolometer pixels that can be fabricated on top of the 512x3 ROIC and that will be reported in a future publication. Several of those pixels have been packaged in the radiometric package in order to characterize their performance. As an example, an NETD as low as 23 mK was measured for a high resistivity pixel packaged in a radiometric package for which the combined transmission of the window and filter are shown in Figure 4 (measurement conditions: flood irradiation with no front optics, f/1, 140 ms integration time, temperature of the detector of 10 C and temperature of the scene of 30 C).
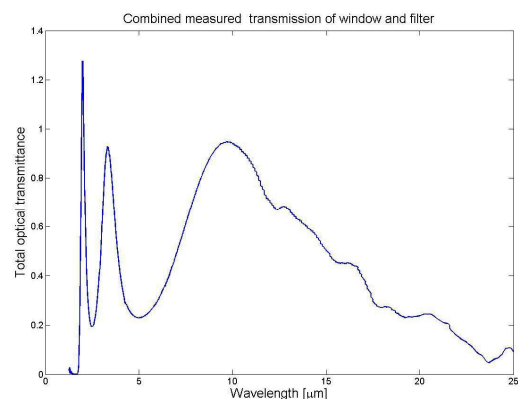

Figure 4: Measured total transmission of the window and the filter of the radiometric package used to package a 512x3 FPA detector with high resistivity pixels for which an NETD of 23 mK was measured (measurement conditions: flood irradiation with no front optics, f/1, 140 ms integration time, temperature of the detector of 10 C and temperature of the scene of 30 C).

3.2 Robustness to Ambient Temperature Variations

Variations in the temperature of the environment of the package induce a variation in the power of the radiation reaching the detector by both heating of the package (direct emission over the detector) and by variation of

the temperature of the objects outside the field of view of the device (variation of the amount of radiation reaching the detector as stray light). In order to assess the radiometric stability of the package, both the robustness to a variation of the ambient temperature (i.e. heating of the package) and to stray radiation (i.e. radiation coming from outside the field of view of the package) need to be studied.

In order to minimize the influence of the variation of the temperature of the package cover on the sensor response, a temperature stabilized radiation shield was placed around the detector (Figure 1). The exterior of the shield as well as the interior of the package cover were plated in gold to minimize heat transfer by radiation between the package cover and the shield. Furthermore, the shield was designed to optimize its temperature control by the TEC.

To characterize the influence of a variation of the temperature of the ambient on the response of the detector a heating tape was placed around the detector cover. The temperature of the package was measured by means of a thermocouple placed on the package cover. The blackbody was set to a fixed temperature of 25 C. Acquisitions were taken while the package was heated. The response of the detector was plotted as a function of the temperature of the package cover. The experimental data was then fitted with a linear fit. The slope of the fitted line represents the variation of the response of the detector per degree of variation of the temperature of the package.

An example of measurement obtained using this method is shown in Figure 5.

The variation of the equivalent temperature of the scene due to a variation of the temperature of the package can be calculated as

$$\frac{\Delta T_{scene}}{\Delta T_{ambient}} \frac{\frac{\Delta \mathrm{Re}\,sponse}{\Delta T_{ambient}}}{SITF}$$

where $\Delta Response/\Delta T_{ambient}$ is the slope of the graph of the response of the detector as a function of the temperature of the package in [counts/C] and the SITF is measured in counts/C.
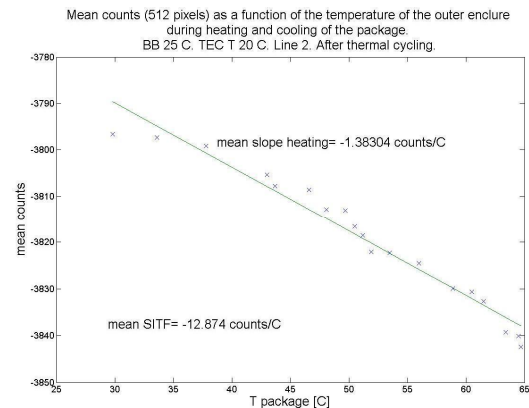

Figure 5: Radiometric stability of a package to a variation of the environment temperature (Type IIB ROIC with low resistivity pixel, 140 ms integration time, 2 MHz clock frequency, TEC T 20 C, BB T 25 C after vibration

From the results shown in Figure 5 it can be calculated that each degree of variation of the temperature of the package will induce a variation of the equivalent temperature of the scene seen by the detector of 0.1 C.

3.3 Robustness to Stray Light

The robustness to the stray light can be understood as variation of the equivalent temperature detected by the sensor per degree of variation of the temperature of the stray light.

The stray light has been represented in the experiment by an extended area blackbody at different temperatures that illuminates the detector outside its field-of-view. During the experiment, the field of view was masked by a mask at 25 C and the variation of the response of the detector with and without the stray light blackbody was measured for different stray light blackbody temperatures.

Figure 6 shows the variation of measured scene temperature due to the presence of the stray light as a function of the temperature of the stray light blackbody.

As it can be seen in Figure 6, the design of the shield has been demonstrated to be very effective in preventing stray radiation from reaching the detector.
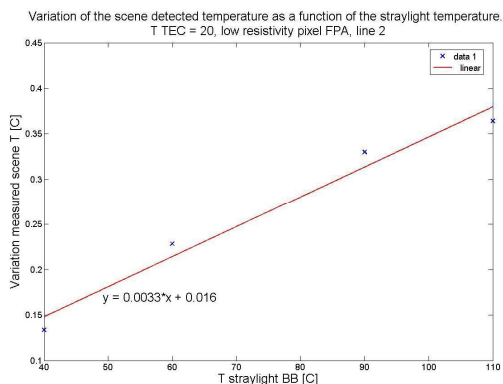
Figure 6: Variation of the measured scene temperature when exposed to the stray light of an extended area blackbody that emits radiation outside the field of view of the package.

3.4 Environmental Tests

The radiometric package was subjected to thermal cycling (MIL-STD-810 method 501) from -55 C to +85 in a dry atmosphere (non-operating) for 30 cycles. Figure 7 shows the thermal cycle used. The length of the cycles was extended in order to ensure a minimum of 20 min soak at each extreme temperature.
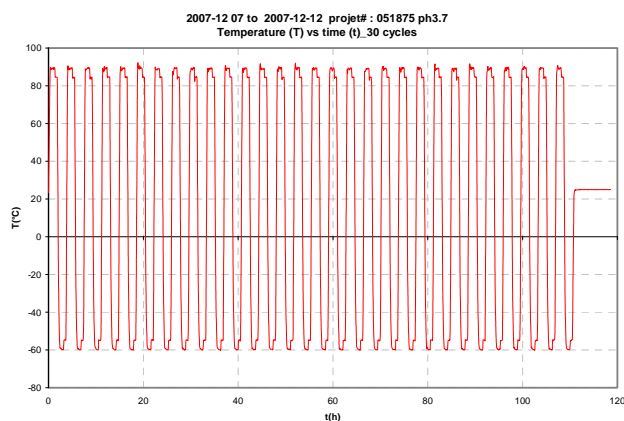

Figure 7: Thermal cycle.

The package was also subjected to severe random vibration in three orthogonal axes according to Table 1. The PSD is a standard GEV-SE curve specified by NASA for small components [9].

Table 1: Random vibration PSD breakpoints

f (Hz)	Amplitude (g2/hz)
20	0.026
50	0.16
800	0.16
2000	0.026
Total	14.1 Grms

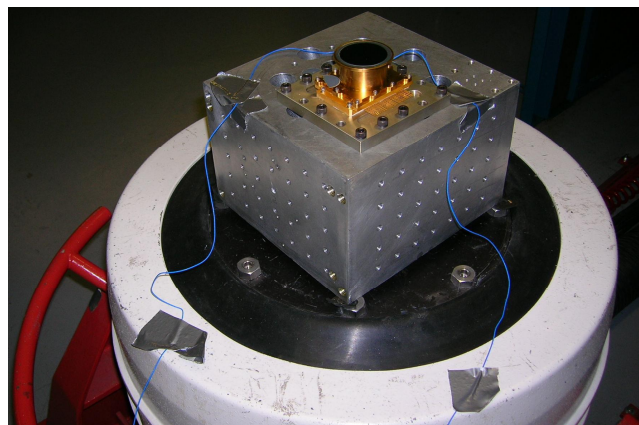A photo of INO's vibration setup is shown in Figure 8.

Figure 8: INO vibration setup.

Finally the device was also subjected to shock according to MIL-STD-810F Method 516.5 at 75 G level, duration of 11 ms 2 pulse per axis.

The performance of the device in terms of NETD and radiometric stability was completely unaltered after the environmental qualification campaign.

4. CONCLUSION

A radiometric package compatible with different microbolometer FPAs has been designed, assembled and fully characterized. The package has been demonstrated with the INO/CSA 512x3 pixel FPA specifically designed for IR pushbroom imaging applications. An NETD as low as 23 mK (broadband filter centered in the 8-12 μm wavelength band, 140 ms integration time, scene temperature of 25 C, detector temperature of 10 C) has been measured for a 512x3 FPA array of high resistance pixels. The package has been shownd to be robust to variations of the ambient temperature and to stray radiation. An environmental testing campaign representative of a space mission has been successfully performed without degradation of the detector performance.

5. REFERENCES

[1] Marraco H., Phong L.N., NIRST, a satellite based IR instrument for fire and sea surface temperature measurement, Proc. SPIE 6213, 62130L, 2006.

[2] Gauvin J., Chateauneuf F., Marchese L., Cote P., Leclerc M., Chevalier C., Marraco H., Pong L.N., Design of the SAC-D/NIRST camera module, Proc. SPIE, 6678, 667814, 2007.

[3] Sen A., Kima Y., Caruso D., Lagerloefd G., Colombb R., Yueha S., Le Vine D., Aquarius/SAC-D Mission overview, Proc. SPIE 6361, 636101I, 2006.

[4] Evans C., Poirier M., Scott A., Touahri D., Ilias S., Doyon R., Design and fabrication of large spectral waveband mirror coatings for scanning Fabry-Perot etalons, Proc. SPIE vol. 7067, 706703, 2008.

[5] Wang M., Asselin D., Topart P, Gauvin J., CGH null test design and fabrication for off-axis aspherical mirror tests, Proc. SPIE 6342, 63421Y, 2007.

[6] Irwin, A., Nicklin, R.L., Standard software for automated testing of infrared imagers, IR windows in practical applications, IEEE Systems Readiness Technology Conference, 1998, pp. 561-571.

[7] Holst G.C., Testing and evaluation of infrared imaging systems, 2nd edition, 1998, page 220.

[8] C.M. Webb, An approach to 3-dimensional noise spectral analysis, Proc. SPIE, vol. 2470, pp. 288-299.

[9] General Environmental Verification Specification for STS & ELV payload, subsystems and components, rev A, NASA Goddard Space Flight Center, June 1996, pp. 2.4-19.